

# ARTIFACT CHARACTERIZATION OF JPEG DOCUMENTS

Pham The Anh, Mathieu Delalandre

Received: 15 March 2017 / Accepted: 7 June 2017 / Published: July 2017

©Hong Duc University (HDU) and Hong Duc University Journal of Science

**Abstract:** *This paper addresses the problem of blocking artifact characterization that is introduced when using low bit-rate JPEG compression. Specifically, a novel blocking metric is presented to characterize the distortion of JPEG blocking artifact when applied to document content. Furthermore, the proposed metric is directly processed in the transform domain without the need of fully decompressing the images, making its computation very time-efficient. Correlation of the proposed metric to OCR performance is validated through our experiments.*

**Keywords:** *Document compression, coding artifact characterization, blocking artifact, ringing artifact.*

## 1. Introduction

The JPEG standard has been widely used for multi-media data compression nowadays. In its essence, the JPEG codec divides input image into non-overlapping  $8 \times 8$  blocks, each of which is then individually compressed by a pipeline of following steps: image de-correlation using Discrete Cosine Transform (DCT), quantization and entropy coding. The DCT coefficients  $F(m, n)$  of an image block  $f(x, y)$  are defined as follows:

$$F(m, n) = \frac{e(m)e(n)}{4} \sum_{x=0}^7 \sum_{y=0}^7 f(x, y) C_{16}^{(2x+1)m} C_{16}^{(2y+1)n} \quad (1)$$

$$\text{where } C_y^x = \cos\left(\frac{x\pi}{y}\right), e(t) = \begin{cases} \frac{1}{\sqrt{2}} & \text{if } t = 0 \\ 1 & \text{otherwise} \end{cases}$$

The inverse DCT transforms (IDCT) is defined to accordingly recover the original image by:

$$f(x, y) = \frac{1}{4} \sum_{m=0}^7 \sum_{n=0}^7 e(m)e(n) F(m, n) C_{16}^{(2x+1)m} C_{16}^{(2y+1)n} \quad (2)$$

At low bit-rate coding, JPEG encoded images are subject to heavy distortion of blocking artifact due to the independent coding of each block. Characterization of blocking

---

Pham The Anh

Faculty of Information and Communication Technologies, Hong Duc University

Email: Phamtheanh@hdu.edu.vn (✉)

Mathieu Delalandre

Computer Science Lab, Francois Rabelais University, Tours city, France

Email: Mathieu.delalandre@univ-tour.fr (✉)

behavior is thus a critical task for various problems including blocking artifact reduction, OCR prediction, adaptive compression, image quality assessment, etc.

Basically, blocking artifact refers to the discontinuities of pixel values along the block boundaries. At low bit-rate coding, the transformed coefficients are heavily quantized resulting in the loss of information of intra-block pixels and of inter-block transitions. Consequently, the decompressed image is annoyed by the discontinuities over the blocks. In the literature, various blocking metrics have been proposed to characterize the blocking artifact for natural images [1]-[7]. However, little attention has been investigated to characterize the blocking distortion for document content.

In this work, we aim at measuring the blocking distortion when using JPEG coding applied to document content. Specifically, the main contribution of this work is three-fold. First, a novel blocking artifact measure is presented to characterize the blocking distortion at low bit-rate compression. Second, we propose computing this measure directly in the DCT domain without decompressing the images. This feature is opposed to many approaches in the literature in which a full decompression stage is obligated [1], [3], [5]-[7]. As such, the characterization becomes time-efficient and could be exploited in a context of adaptive compression or artifact post-processing optimization. At last, we show by experimental results the relevance of the proposed blocking measure to OCR performance.

The rest of this paper is structured into five sections. Section II reviews the key methods for blocking artifact characterization in the literature. Section III presents a technique to efficiently compute block boundary variation in the transform domain. The proposed blocking measure is described in Section IV. Experimental results are provided in Section V and we conclude the paper in Section VI.

## 2. Review of blocking artifact characterization

A number of blocking metrics have been proposed to characterize the image degradation caused by low bit-rate compression. Most of these metrics were conducted in the image spatial domain [1], [3], [5]-[8], while several attempts proposed computing blocking measure directly in DCT domain [2], [4], [9], [10].

In [1], a blocking measure was estimated by counting the number of zero-valued DCT coefficients. To differentiate the naturally uniform regions from the uniform areas caused by blocking artifact, the number of zero-valued coefficients is weighted using a quality relevance map which is computed based on the slope of the Fourier magnitude spectrum of the blurred image. A small value of the slope indicates the presence of naturally uniform regions. The authors in [3] detect blocking candidates by measuring the abrupt changes at the block boundaries. Doing so, true edge blocks are also included in the candidate list but they are then filtered out based on the observation that the intensity values are often mutually different on the edge boundary. Blocking strength is finally estimated from the remaining candidates by averaging the sums of horizontal masked cross-block-boundary difference (SHMCD).

While all the aforementioned methods are dedicated to measure blocking artifact in the spatial domain, several attempts have been investigated to detect blockiness distortion directly in the DCT transform [2], [4], [9], [10]. Blockiness processing in the DCT domain brings great benefit of efficient computation as it avoids applying IDCT transform which is too costly. One of the earliest blocking metrics was proposed in [9] so-called mean squared difference of slope (MSDS). In its essence, MSDS is computed as the mean square difference between the gradient computed at a horizontal/vertical boundary of a block and the average gradient computed from the adjacent slopes along that boundary.

It is worth mentioning that all these blocking metrics are devoted to natural images. There has been little discussion about the behavior of blocking artifact for document images. To our best of knowledge, only the work in [11] provided a preliminary evaluation of JPEG, JPEG 2000 and MRC coding methods using the PSNR metric using a few document samples. In the following sections, we attempt to bring a novel and efficient metric for measuring blocking distortion dedicated to document content.

### 3. Computing block boundary variation in DCT domain

Given an image  $f$  having the size of  $M \times N$ , let  $B_x$  and  $B_y$  be the number of blocks in the vertical and horizontal directions (i.e.,  $B_x = \left\lceil \frac{M}{8} \right\rceil$  and  $B_y = \left\lceil \frac{N}{8} \right\rceil$ ). For the sake of presentation, we denote a block located at  $k^{th}$  row and  $l^{th}$  column by  $(k,l)$  with  $k = 0, 1, \dots, B_x - 1$  and  $l = 0, 1, \dots, B_y - 1$ . We also denote  $F^{k,l}(m,n)$  as the DCT coefficients of the block  $(k,l)$  with  $m, n \in \{0, 1, \dots, 7\}$ . Since blocking artifact causes the abrupt changes in pixel intensity at the block boundaries, it makes sense to analyze the variation along the boundaries of the blocks. Specifically, we suggest computing block boundary variation (BBV) for each block by dividing the block into 16 subregions (Figure 1).

$S_{00}^{k,l}$	...		$S_{03}^{k,l}$	$S_{00}^{k,l+1}$	...		$S_{03}^{k,l+1}$
$\vdots$				$\vdots$			
$S_{30}^{k,l}$			$S_{33}^{k,l}$	$S_{30}^{k,l+1}$			$S_{33}^{k,l+1}$
$S_{00}^{k+1,l}$	...		$S_{03}^{k+1,l}$				
$\vdots$							

Figure 1. Computing block boundary variation at  $2 \times 2$  super-pixel level

Each subregion is regarded as a super-pixel corresponding to a local window having the size of  $2 \times 2$ . Each super-pixel  $(u, v)$  is assigned with an average intensity value  $S_{uv}^{k,l} (u, v \in \{0, 1, 2, 3\})$  computed by [12]:

$$S_{uv}^{k,l} = \frac{1}{4} \sum_{i=0}^1 \sum_{j=0}^1 f^{k,l}(2u+i, 2v+j) \quad (3)$$

Where  $f^{k,l}(x, y)$  is the intensity value of the pixel  $(x, y)$  in the block  $(k, l)$  of the image  $f$ .

For each block  $(k, l)$ , we define  $BBV_H(f^{k,l})$  and  $BBV_V(f^{k,l})$  as horizontal and vertical block boundary variation, respectively. These measures are computed as follows:

$$BBV_H(f^{k,l}) = \sum_{i=0}^3 |S_{i0}^{k,l+1} - S_{i3}^{k,l}|$$

$$BBV_V(f^{k,l}) = \sum_{i=0}^3 |S_{0i}^{k+1} - S_{3i}^{k,l}|$$

In what follows, we investigate a means for fast computing BBV in the DCT domain. The following materials are targeted to computing  $BBV_H(f^{k,l})$  although the same process can be applied to compute  $BBV_V(f^{k,l})$ .

Firstly, substituting (2) into (3) and rearranging the terms in a similar manner as given in [12], we obtain the following expression:

$$S_{uv}^{k,l} = \sum_{m=0}^7 \sum_{n=0}^7 F^{k,l}(m, n) w_{uv}(m, n) \quad (4)$$

$$\text{where } w_{uv}(m, n) = \frac{1}{4} e(m) e(n) C_{16}^m C_8^{(2u+1)m} C_{16}^n C_8^{(2v+1)n}.$$

For simplification purpose, we define  $D_i$  with  $i \in \{0, 1, 2, 3\}$  as the sub-terms of  $BBV_H(f^{k,l})$ :  $D_i = S_{i0}^{k,l+1} - S_{i3}^{k,l}$ . Accordingly,  $D_0$  is represented in the form of:

$$\begin{aligned} D_0 &= S_{00}^{k,l+1} - S_{03}^{k,l} \\ &= \sum_{m=0}^7 \sum_{n=0}^7 (F^{k,l+1}(m, n) w_{00}(m, n) - F^{k,l}(m, n) w_{03}(m, n)) \\ &= \sum_{m=0}^7 \sum_{n=0}^7 \frac{e(m) e(n) C_{16}^m C_{16}^m C_8^m}{4} (F^{k,l+1}(m, n) C_8^n - F^{k,l}(m, n) C_8^{7n}) \end{aligned}$$

Note that  $C_8^{7n} = (-1)^n C_8^n$ , we obtain:

$$D_0 = \frac{1}{4} \sum_{m=0}^7 \sum_{n=0}^7 e(m) e(n) C_{16}^m C_{16}^m C_8^m C_8^n R(m, n)$$

where  $R(m, n) = F^{k,l+1}(m, n) - (-1)^n F^{k,l}(m, n)$ . In the same manner, the remaining  $D_i$  are computed by  $1 \leq i \leq 3$ :  $D_i = \frac{1}{4} \sum_{m=0}^7 \sum_{n=0}^7 e(m) e(n) C_{16}^m C_{16}^m C_8^{(2i+1)m} C_8^n R(m, n)$

Let  $z_k(m, n) = \frac{1}{4}e(m)e(n)C_{16}^n C_{16}^m C_8^{km} C_8^n$  with  $k \in \{1, 3, 5, 7\}$ , due to the fact that  $C_8^{5n} = (-1)^n C_8^{3n}$ , the following properties are derived for  $z_k(m, n)$ :

- $\frac{z_7(m, n)}{z_1(m, n)} = \frac{z_5(m, n)}{z_3(m, n)} = (-1)^m$
- $k_m = \frac{z_3(m, n)}{z_1(m, n)} = \frac{C_8^{3m}}{C_8^m}$  (see Table 1)
- $z_k(m, n) = 0$  for either  $m = 4$  or  $n = 4$

As each  $D_i$  is composed of symmetric terms, we can unroll  $D_i$  by defining  $G_3^{odd}$  and  $G_3^{even}$  with  $j \in \{0, 1\}$  as follows:  $G_j^{odd} = \sum_{m=1,3,5,7} \sum_{n=0}^7 z_{2j+1}(m, n)R(m, n)$ .

$$G_j^{even} = \sum_{m=0,2,6} \sum_{n=0}^7 z_{2j+1}(m, n)R(m, n)$$

As a result, each  $D_i$  is represented in the form of:

$$\begin{aligned} D_0 &= G_0^{even} + G_0^{odd} \\ D_1 &= G_1^{even} + G_1^{odd} \\ D_2 &= G_1^{even} - G_1^{odd} \\ D_3 &= G_0^{even} - G_0^{odd} \end{aligned}$$

**Table 1.** Precomputation of  $k_m$

m	0	1	2	3	5	6	7
$k_m$	1	$\frac{C_8^3}{C_8^1}$	-1	$-\frac{C_8^1}{C_8^3}$	$\frac{C_8^1}{C_8^3}$	-1	$-\frac{C_8^3}{C_8^1}$

If the property of  $k_m$  in Table 1 is taken into account, we can further simplify the computation of  $G_1^{even}$  and  $G_1^{odd}$  by:

$$\begin{aligned} G_1^{even} &= \sum_{n=0}^7 (z_1(0, n)R(0, n) - z_1(2, n)R(2, n) - z_1(6, n)R(6, n)) \\ G_1^{odd} &= \sum_{n=0}^7 (k_1 z_1(1, n)R(1, n) + k_3 z_1(3, n)R(3, n) - k_3 z_1(5, n)R(5, n) - k_1 z_1(7, n)R(7, n)) \\ &= k_1 \sum_{n=0}^7 z_1(1, n)R(1, n) - k_1 \sum_{n=0}^7 z_1(7, n)R(7, n) + k_3 \sum_{n=0}^7 z_1(3, n)R(3, n) - k_3 \sum_{n=0}^7 z_1(5, n)R(5, n) \end{aligned}$$

To compute  $D_i$  efficiently, we define  $H_t$  with  $t \in \{0, 1, 2, 3, 5, 6, 7\}$  by:

$$H_t = \sum_{n \in \{0, 1, 2, 3, 5, 6, 7\}} z_1(t, n)R(t, n)$$

With these results in mind,  $D_i$  can be finally computed by:

$$D_0 = H_0 + H_2 + H_6 + (H_1 + H_3 + H_5 + H_7)$$

$$D_3 = H_0 + H_2 + H_6 - (H_1 + H_3 + H_5 + H_7)$$

$$D_1 = H_0 - (H_2 + H_6) + k_1(H_1 - H_7) + k_3(H_3 - H_5)$$

$$D_2 = H_0 - (H_2 + H_6) - (k_1(H_1 - H_7) + k_3(H_3 - H_5))$$

In short, computation of  $BBV_H(f^{k,l})$  requires 51M + 106A. This complexity is much more efficient than applying full IDCT (i.e., 4096M + 4096A) even when comparing with fast IDCT.

#### 4. Document blocking artifact measure (DBAM)

In general, blocking artifact causes the abrupt changes at the boundaries of the blocks. Hence, measuring the changes along the block boundaries is a good indication of blocking artifact. However, since document content is mostly composed of two-intensity values, the transition between foreground (FG) and background (BG) would cause the abrupt changes as well. This occurs when parts of the characters' strokes are located at the boundaries of the blocks (see the characters 'P', 'H', and 'L' for example). To correctly estimate the blocking artifact measure, it is desired to differentiate the abrupt changes caused by the natural FG/BG transition from the changes introduced by blocking artifact. We propose handling this matter based on the following two observations.

First, since the size of each character is likely to be much higher than the conventional block size (i.e.,  $8 \times 8$ ), each character can be considered as a region composing of several blocks. Therefore, it is occasionally the case that all four boundaries of one block contain the strokes of the characters. In contrary, at low bit-rate coding, the abrupt changes caused by blocking artifact are likely to occur along all the block boundaries since each block is independently encoded.

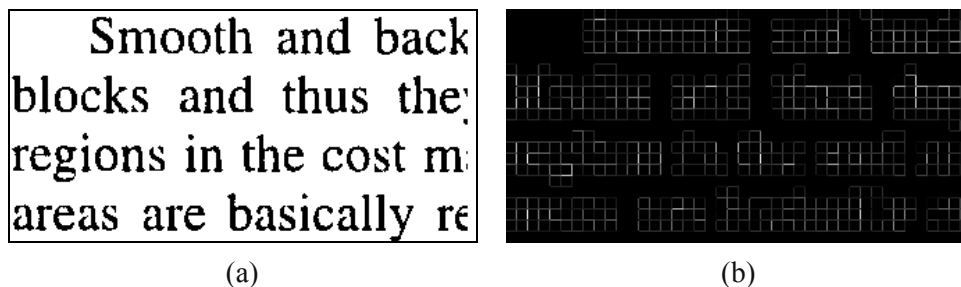


**Figure 2.** (a) Original image; (b) BBV strength map (higher values, brighter pixels) with JPEG quality factor = 2

Figure 2 plots the BBV strength map (JPEG quality = 2) where one can see the boundary discontinuities virtually occur at all the boundaries of foreground blocks. For original or high bit-rate coding image, the boundary discontinuities partially occur at the block

boundaries with a much lower frequency. Consequently, one can exploit the BBV distribution at four boundaries of each block to eliminate the contribution caused by the FG/BG transition at that block. This can be simply done by weighting each block by the ratio of the smallest value to the biggest one among four BBV measures of the block.

Second, it was found that the BBV peaks are likely to occur at the areas corresponding to the natural FG/BG transitions. This observation suggests that using a high-band filter seems to be a good solution to eliminate the BBV peaks at these regions. Such a technique, however, requires a good threshold selection step which is not easily handled. Alternatively, we propose using a non-linear filter to address this problem. The rationale is again based on the fact that the BBV map of a low bit-rate coding image is distributed more uniformly than that of a high bit-rate coding image. Therefore, a non-linear filtering technique such as median filtering would help eliminate the outliers corresponding to the BBV peaks caused by the FG/BG transitions. Specifically, we construct a circular masking filter  $M_{k,l}(r)$  centered at the block  $(k,l)$  with the radius  $r$  as shown in Figure 3.

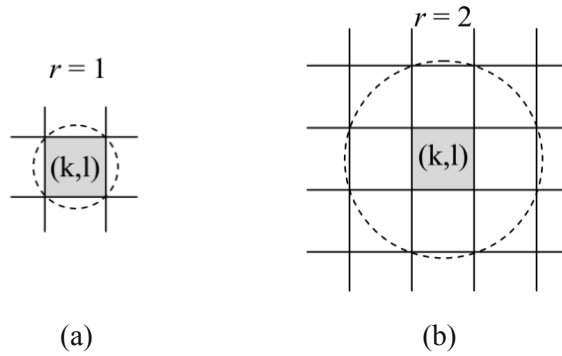


**Figure 3.** Non-linear mask filtering: (a) radius = 1, (b) radius = 2

Accordingly,  $M_{k,l}(1)$  and  $M_{k,l}(2)$  contain 4 and 12 BBV elements, respectively. Next, we define a blockiness measure,  $BM_{k,l}$ , for the block  $(k,l)$  by the weighted median value among all the BBV values positioning inside the mask  $M_{k,l}(r)$ . In our experiments, we set the parameter  $r = 2$ .

For completeness, the procedure to compute the blockiness measure is sketched out as follows:

- Compute  $BBV_V$  and  $BBV_H$  for all the boundaries of the blocks.
- Compute a weight  $\alpha_{k,l}$  for each block  $(k,l)$  by:

$$\alpha_{k,l} = \frac{\min_{i \in M_{k,l}(1)} \{BBV_i\}}{\max_{i \in M_{k,l}(1)} \{BBV_i\}}$$

- Compute the blockiness measure  $BM_{k,l}$  for each block  $(k,l)$  by:

$$BM_{k,l} = \alpha_{k,l} MED_{i \in M_{k,l}(2)} \{BBV_i\}$$

where  $MED\{X\}$  is the median value of the list  $X$ .

- Compute the document blocking artifact measure (DBAM):

$$DBAM = \frac{1}{|U|} \sqrt{\sum_{(k,l) \in U} BM_{k,l}^2}$$

where  $U$  is the set of all image blocks.

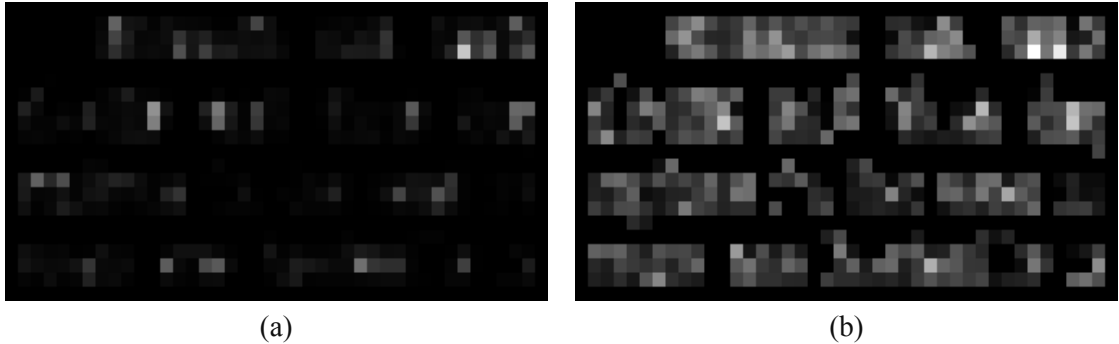


**Figure 4.** Blockiness measure ( $BM$ ) map for the image in Figure 2 (higher values, brighter pixels): (a) JPEG quality = 20; (b) JPEG quality = 2

Figure 4 illustrate the  $BM_{k,l}$  maps for all the blocks of the image in Figure 2 in which the JPEG quality factor is first set to 20 and then 2. As can be seen in Figure 4(b), when encoding the image at low bit-rate, most of the foreground blocks are disturbed by blocking artifact. To obtain a global evaluation for the entire image, we define a document blocking artifact measure (DBAM) as the mean square root of all the  $BM_{k,l}$ .

## 5. Experimental results

### 5.1. Dataset and experimental settings

The proposed DBAM metric is evaluated for a wide range of bit-rate coding in accordance with the OCR performance. For this purpose, the software ABBYY FineReader 12.0<sup>1</sup> is employed to compute the OCR results. Specifically, OCR accuracy is computed as the ratio of the number of correctly recognized characters to the total characters in the groundtruth. We used the dataset Medical Archive Records (MAR) for OCR recognition from U.S.National Library of Medecine<sup>2</sup>. This dataset contains real documents which are scanned from different types of biomedical journals. Each document contains several zones accompanying with corresponding groundtruth information. For simplification, each zone is independently treated as an image along with its corresponding groundtruth, resulting in 296 images in total. Each image is encoded at 16

<sup>1</sup> <http://finereader.abbyy.com/professional/features/>

<sup>2</sup> <http://marg.nlm.nih.gov/>

JPEG compression qualities (i.e.,  $\{1,2,\dots,16\}$ ). From the compressed images, the bit-rates are computed and these was found that the obtained bit-rates vary in the range of  $[0.1,1.1]$ . All the experiments are performed on the following machine configuration: Windows 7 (64-bit), Intel Core i7 (2.1 GHz), 16Gb RAM.

## 5.2. DBAM characterization results

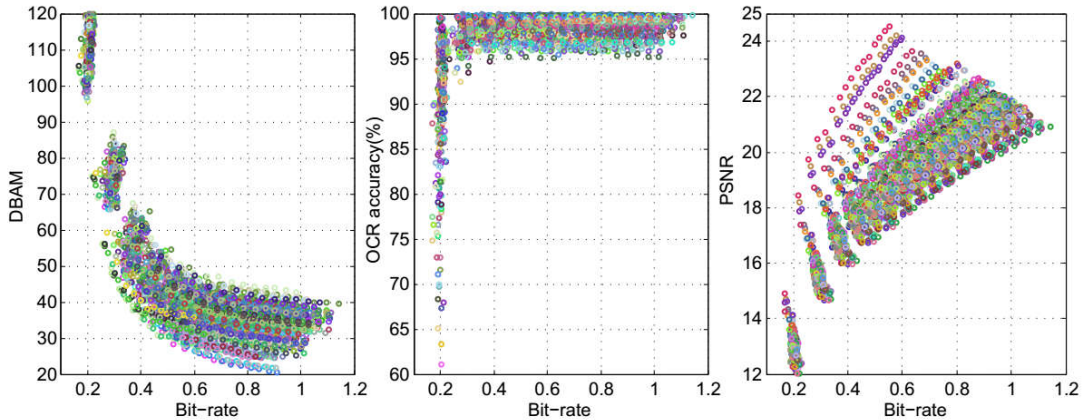


**Figure 5.** DBAM, OCR accuracy and PSNR for 296 images

Figure 5 presents DBAM results, OCR accuracy and PSNR results over the bit-rates for all the images in the dataset. The common range of DBAM values is in  $[10,120]$  (i.e., the smaller the DBAM, the lower the blocking distortion). As can be seen, the DBAM curves have quite similar behavior (i.e., the marginal slope) for all the images. Specifically, the marginal slopes of DBAM values are quite sharp at low bit-rates (i.e.,  $[0.15,0.3]$ ) and tend to be gradually stable afterward. The same remark is extracted for the OCR accuracy in which high DBAM values correspond to low OCR performance. Also, OCR results start to be less sensitive to blocking artifact when the bit-rate  $> 0.3$ . Consequently, it seems that the correlation between DBAM and OCR results is non-linear, but they can be well represented by piecewise functions of the bit-rate. To be more precise, the first parts of DBAM and OCR results are very linearly correlated up to a specific limit of the bit-rate (e.g., bit-rate  $< 0.4$ ). However, this degree of linear dependence is greatly dropped when the bit-rate is sufficiently high since both DBAM measure and OCR performance can be virtually modeled by two constant functions.

To validate these propositions, we computed the Pearson correlation coefficient (PCC) between DBAM and OCR results for two intervals of the bit-rate:  $[0.1,0.4)$  and  $[0.4,1.1]$ . The range of PCC is well-defined in the interval of  $[-1,1]$  with the senses that perfect linear correlation has the corresponding PCC of 1 (positive correlation) or  $-1$  (negative correlation), and no correlation corresponds to a PCC value of 0. The obtained PCC results are  $-0.9583$  and  $-0.2635$  with respect to the bit-rate intervals  $[0.1,0.4)$  and  $[0.4,1.1]$ . In other words, the

DBAM and OCR results are highly (linear) correlated at low bit-rates and less dependent at high bit-rates.

For comparative evaluation, we computed the peak signal-to-noise ratio (PSNR) between the decompressed images and the original ones. PSNR is a common criterion for measuring image quality of natural images, especially in the domain of image compression, reconstruction and denoising. As can be seen in Figure 5.1, PSNR values are in the range of [10,25] (i.e., higher PSNR, better image quality) and have relative high dispersion for the bit-rates in [0.3,0.8]. In addition, we also computed the correlations of PSNR and DBAM to OCR results for the bit-rates in [0.1,1.1]. Accordingly, the obtained PCC values are 0.7191 and -0.8729. That said, PSNR is reasonably and positively correlated to OCR accuracy, whereas DBAM is highly and negatively correlated to OCR results.

## 6. Conclusions

A novel and efficient approach has been presented to compute the blocking artifact measure for document content. In contrast to previous work, the proposed DBAM measure is directly computed in the DCT domain and is dedicated to estimate JPEG artifact distortion when applied to document images. Experiments showed that DBAM is highly correlated to OCR performance and is extremely efficient. Future work would be targeted to optimal document image decompression.

## References

- [1] S. Golestaneh and D. Chandler (2014), *No-reference quality assessment of jpeg images via a quality relevance map*, Signal Processing Letters (SPL), vol. 21, no. 2, pp. 155-158.
- [2] C. Park, J. Kim, and S. Ko (2007), *Fast blind measurement of blocking artifacts in both pixel and dct domains*, Journal of Mathematical Imaging and Vision, vol. 28, no.3, pp. 279-284.
- [3] S. Lee and S. J. Park (2012), *A new image quality assessment method to detect and measure strength of blocking artifacts*, Signal Processing: Image Communication, vol. 27, no. 1, pp. 31 - 38.
- [4] S. Liu and A. Bovik (2002), *Efficient dct-domain blind measurement and reduction of blocking artifacts*, Transactions on Circuits and Systems for Video Technology (TCSVT), vol. 12, no. 12, pp. 1139-1149.
- [5] F. Pan, X. Lin, S. Rahardja, E. Ong, and W. Lin (2007), *Using edge direction information for measuring blocking artifacts of images*, Multidimensional Systems and Signal Processing (MSSP), vol. 18, no. 4, pp. 297-308.
- [6] F. Yan, S. Wan, Y. Chang, and Z. Luo (2006), *A no-reference blocking artifact metric for b-dct video*, Journal of Zhejiang University SCIENCE A, vol. 7, no. 1, pp. 95-100, 2006.

- [7] L. Meesters and J. Martens (2002), *A single-ended blockiness measure for jpeg-coded images*, Signal Processing, vol. 82, no. 3, pp. 369-387.
- [8] S. Suthaharan (2009), *No-reference visually significant blocking artifact metric for natural scene images*, Signal Processing, vol. 89, no. 8, pp. 1647-1652.
- [9] S. Minami and A. Zakhor (1995), *An optimization approach for removing blocking effects in transform coding*, Circuits and Systems for Video Technology, IEEE Transactions on, vol. 5, no. 2, pp. 74-82.
- [10] G. Triantafyllidis, D. Tzovaras, and M. Strintzis (2002), *Blocking artifact detection and reduction in compressed data*, Transactions on Circuits and Systems for Video Technology (TCSVT), vol. 12, no. 10, pp. 877-890.
- [11] M. Barni (2006), *Document and Image Compression*. CRC Press.
- [12] H. S. Chang and K. Kang (2005), *A compressed domain scheme for classifying block edge patterns*, IEEE Transactions on Image Processing, vol. 14, no. 2, pp. 145-151, Feb 2005.